Journal of
Composites Science

MDPI

Article

Study on the Melting Temperature, the Jumps of Volume, Enthalpy and Entropy at Melting Point, and the Debye Temperature for the BCC Defective and Perfect Interstitial Alloy WSi under Pressure

Hoc Nguyen Quang [1], Hien Nguyen Duc [2], Dung Nguyen Trong [3,*], Van Cao Long [3] and Ştefan Ţălu [4,*]

[1] Faculty of Physics, Hanoi National University of Education, 136 Xuan Thuy, Hanoi 100000, Vietnam; hocnq@hnue.edu.vn
[2] Mac Dinh Chi High School, Gia Lai Province 61000, Vietnam; n.duchien@gmail.com
[3] Institute of Physics, University of Zielona Góra, Prof. Szafrana 4a, 65-516 Zielona Góra, Poland; caolongvanuz@gmail.com
[4] The Directorate of Research, Development and Innovation Management (DMCDI), Technical University of Cluj-Napoca, 15 Constantin Daicoviciu St., Cluj-Napoca, 400020 Cluj County, Romania
* Correspondence: dungntsphn@gmail.com (D.N.T.); stefan.talu@auto.utcluj.ro (Ş.Ţ.)

Abstract: The objective of this study is to determine the analytic expressions of the Helmholtz free energy, the equilibrium vacancy concentration, the melting temperature, the jumps of volume, enthalpy the mean nearest neighbor distance and entropy at melting point, the Debye temperature for the BCC defective, the limiting temperature of absolute stability for the crystalline state, and for the perfect binary interstitial alloy. The results obtained from the expressions are combined with the statistical moment method, the limiting condition of the absolute stability at the crystalline state, the Clausius–Clapeyron equation, the Debye model and the Gruneisen equation. Our numerical calculations of obtained theoretical results were carried out for alloy WSi under high temperature and pressure. Our calculated melting curve and relation between the melting temperature and the silicon concentration for WSi are in good agreement with other calculations. Our calculations for the jumps of volume, enthalpy and entropy, and the Debye temperature for WSi predict and orient experimental results in the future.

Keywords: statistical moment method; defective and perfect interstitial alloy WSi; equilibrium vacancy concentration; jumps of volume; enthalpy and entropy at melting point

Citation: Quang, H.N.; Duc, H.N.; Trong, D.N.; Long, V.C.; Ţălu, Ş. Study on the Melting Temperature, the Jumps of Volume, Enthalpy and Entropy at Melting Point, and the Debye Temperature for the BCC Defective and Perfect Interstitial Alloy WSi under Pressure. *J. Compos. Sci.* **2021**, *5*, 153. https://doi.org/10.3390/jcs5060153

Academic Editor: Konda Gokuldoss Prashanth

Received: 4 May 2021
Accepted: 3 June 2021
Published: 7 June 2021

1. Introduction

Metals and interstitial alloys [1–5] have been investigated by several research groups in the last decades due to their applications in various fields [6–9]. Many theoretical and experimental studies about the mechanical and thermodynamic properties of metals and interstitial alloys gained scientific and technological attention and represent an active area of research that requires integrating modern scientific insights [10–14] from multiple disciplines [15–19].

Different researchers have studied the dependence of the mechanical and thermodynamic properties of materials on the temperature (T), pressure (P), and concentration of components for these materials. It is known that point defects such as vacancies have important contributions to the properties of materials [18–24]. At the melting point, the equilibrium vacancy concentration of metals changes from 10^{-4} to 10^{-2} [20]; therefore, it has a significant influence on the thermodynamic quantities of crystals at high temperatures. W has very high melting temperatures and can provide fundamental information on the equilibrium vacancy concentrations in metals and alloy metals with structured Body-Centered-Cubic (BCC) and their temperature dependences [20–22]. At P = 0.1 MPa,

W has a BCC structure with lattice constant (a), a = 3.1649 × 10^{-10} m at T = 300 K and a melting point at T = 3690 K. The melting curve of W was studied by the optical method at P = 5 GPa and T = (4050 ± 200) K with dT/dP = 75 K/GPa [25] and up to P = 90 GPa and T ~ (4000 ± 100) K using the Laser-Heated Diamond Anvil Cell (LHDAC) for optical measurements [26].

In various studies, researchers determined the melting temperature (T_m) of a crystal only from the solid phase and applied the statistical moment method (SMM) [27–33]. From the SMM method, the stability temperature (T_S) can be determined at different pressures, and the corresponding calculations to find T_m from T_S, and then T_S at crystalline state is defined by $\left(\frac{\partial P}{\partial V}\right)_{T_s} = 0$. Then, the isothermal compressibility of the crystal is equal to infinite. Several SMM calculations are more consistent with experiments than those obtained from other calculations.

In this research, the melting temperature, the jumps of volume, enthalpy and entropy at the melting point, and the Debye temperature for the BCC defective and perfect binary interstitial alloy by combining the SMM, the limiting condition of the absolute stability of the crystalline state, the Clapeyron-Clausius equation, the Debye model and the Gruneisen equation are studied. The theoretical results are numerically performed for alloy WSi, and some of our calculated results are compared with experiments and other calculations.

2. Content of Research

2.1. Melting Temperature, Jumping of Volume, Enthalpy and Entropy at Melting Point, and Debye Temperature of the BCC Defective and Perfect Binary Interstitial Alloy

In our model, the interstitial alloy AB with the concentration $c_B << c_A$, was applied. In it, the A metal has atoms in the center and peaks of cubic, while the atoms of B are in the center of cubic. With the parameters $k, \gamma_1, \gamma_2, \gamma$, the cohesive energy u_0 with the sphere center at the position of B, radii r_{1B} and r_{2B} are determined as follows [1–4,29,33]:

$$u_{0B} = \frac{1}{2}\sum_{i=1}^{n_i}\varphi_{AB}(r_i) = \varphi_{AB}(r_{1B}) + 2\varphi_{AB}(r_{2B}), r_{2B} = \sqrt{2}r_{1B}, \tag{1}$$

$$k_B = \frac{1}{2}\sum_i\left(\frac{\partial^2\varphi_{AB}}{\partial u_{i\beta}^2}\right)_{eq} = \frac{1}{r_{1B}}\frac{d\varphi_{AB}(r_{1B})}{dr_{1B}} + \frac{d^2\varphi_{AB}(r_{2B})}{dr_{2B}^2} + \frac{1}{r_{2B}}\frac{d\varphi_{AB}(r_{2B})}{dr_{2B}}, \tag{2}$$

$$\gamma_B = 4(\gamma_{1B} + \gamma_{2B}), \tag{3}$$

$$\gamma_{1B} = \frac{1}{48}\sum_i\left(\frac{\partial^4\varphi_{AB}}{\partial u_{i\beta}^4}\right)_{eq} = \frac{1}{24}\frac{1}{8r_{1B}^2}\frac{d^2\varphi_{AB}(r_{1B})}{dr_{1B}^2} - \frac{1}{8r_{1B}^3}\frac{d\varphi_{AB}(r_{1B})}{dr_{1B}} + \frac{1}{48}\frac{d^4\varphi_{AB}(r_{2B})}{dr_{2B}^4} + \frac{1}{8r_{2B}}\frac{d^3\varphi_{AB}(r_{2B})}{dr_{2B}^3} - \frac{5}{16r_{2B}^2}\frac{d^2\varphi_{AB}(r_{2B})}{dr_{2B}^2} + \frac{5}{16r_{2B}^3}\frac{d\varphi_{AB}(r_{2B})}{dr_{2B}}, \tag{4}$$

$$\gamma_{2B} = \frac{6}{48}\sum_i\left(\frac{\partial^4\varphi_{AB}}{\partial u_{i\alpha}^2\partial u_{i\beta}^2}\right)_{eq} = \frac{1}{4r_{1B}^2}\frac{d^2\varphi_{AB}(r_{1B})}{dr_{1B}^2} - \frac{1}{4r_{1B}^3}\frac{d\varphi_{AB}(r_{1B})}{dr_{1B}} + \frac{1}{8}\frac{d^4\varphi_{AB}(r_{2B})}{dr_{2B}^4} + \frac{1}{4r_{2B}}\frac{d^3\varphi_{AB}(r_{2B})}{dr_{2B}^3} + \frac{7}{8r_{2B}^2}\frac{d^2\varphi_{AB}(r_{2B})}{dr_{2B}^2} - \frac{7}{8r_{2B}^3}\frac{d\varphi_{AB}(r_{2B})}{dr_{2B}}, \tag{5}$$

where $u_{i\beta}$, n_i, and $r_{1B} = r_{01B} + y_{0A_1}(T)$ are the displacements of the ith atom in the direction of $\beta, \alpha, \beta = x, y, z, \alpha \neq \beta$, the number of atoms on the ith coordination sphere with radius $r_i (i = 1, 2)$, and the nearest neighbor distance between the interstitial atom B and the main metal A in the alloy at temperature T; $y_{0A_1}(T)$ and r_{01B} are the displacements of atom A_1 (atom A in the body center of the cubic unit cell) from the equilibrium position at temperature T, determined from the minimum condition of the cohesive energy u_{0B}, and the nearest neighbor distance between the interstitial atom B and the main metal A in the alloy at temperature 0 K; φ_{AB} is the interaction potential between atom A and atom B. The

cohesive energy u_0 and the alloy parameters $k, \gamma_1, \gamma_2, \gamma$ for atom A_1 (atom A in the body center of the cubic unit cell) in the approximation of three coordination spheres with the sphere center at the position of A_1 and the radius r_{1A_1} of the third coordination sphere are determined as follows [1–4,29,33]:

$$u_{0A_1} = u_{0A} + \varphi_{AB}(r_{1A_1}), \tag{6}$$

$$k_{A_1} = k_A + \frac{1}{2}\sum_i \left[\left(\frac{\partial^2 \varphi_{AB}}{\partial u_{i\beta}^2}\right)_{eq}\right]_{r=r_{1A_1}} = k_A + \frac{d^2\varphi_{AB}(r_{1A_1})}{dr_{1A_1}^2} + \frac{2}{r_{1A_1}}\frac{d\varphi_{AB}(r_{1A_1})}{dr_{1A_1}}, \tag{7}$$

$$\gamma_{A_1} = 4(\gamma_{1A_1} + \gamma_{2A_1}), \tag{8}$$

$$\gamma_{1A_1} = \gamma_{1A} + \frac{1}{48}\sum_i \left[\left(\frac{\partial^4 \varphi_{AB}}{\partial u_{i\beta}^4}\right)_{eq}\right]_{r=r_{1A_1}} = \gamma_{1A} + \frac{1}{24}\frac{d^4\varphi_{AB}(r_{1A_1})}{dr_{1A_1}^4} + \frac{1}{4r_{1A_1}^2}\frac{d^2\varphi_{AB}(r_{1A_1})}{dr_{1A_1}^2} - \frac{1}{4r_{1A_1}^3}\frac{d\varphi_{AB}(r_{1A_1})}{dr_{1A_1}}, \tag{9}$$

$$\gamma_{2A_1} = \gamma_{2A} + \frac{6}{48}\sum_i \left[\left(\frac{\partial^4 \varphi_{AB}}{\partial u_{i\alpha}^2 \partial u_{i\beta}^2}\right)_{eq}\right]_{r=r_{1A_1}} = \gamma_{2A} + \frac{1}{2r_{1A_1}}\frac{d^3\varphi_{AB}(r_{1A_1})}{dr_{1A_1}^3} - \frac{3}{4r_{1A_1}^2}\frac{d^2\varphi_{AB}(r_{1A_1})}{dr_{1A_1}^2} + \frac{3}{4r_{1A_1}^3}\frac{d\varphi_{AB}(r_{1A_1})}{dr_{1A_1}}, \tag{10}$$

where $r_{1A_1} \approx r_{1B}$ is the nearest neighbor distance between atom A_1 and the other atoms in the alloy.

The $u_0, k, \gamma_1, \gamma_2, \gamma$ are the cohesive energy and the alloy parameters for atom A_2 (atom A in the peaks of the cubic unit cell) in the approximation of three coordination spheres, with A_2 and radius r_{1A_2} of the third coordination sphere as follows [1–4,29,33]:

$$u_{0A_2} = u_{0A} + \varphi_{AB}(r_{1A_2}), \tag{11}$$

$$k_{A_2} = k_A + \frac{1}{2}\sum_i \left[\left(\frac{\partial^2 \varphi_{AB}}{\partial u_{i\beta}^2}\right)_{eq}\right]_{r=r_{1A_2}} = k_A + 2\frac{d^2\varphi_{AB}(r_{1A_2})}{dr_{1A_2}^2} + \frac{4}{r_{1A_2}}\frac{d\varphi_{AB}(r_{1A_2})}{dr_{1A_2}}, \tag{12}$$

$$\gamma_{A_2} = 4(\gamma_{1A_2} + \gamma_{2A_2}), \tag{13}$$

$$\gamma_{1A_2} = \gamma_{1A} + \tfrac{1}{48}\sum_i \left[\left(\frac{\partial^4 \varphi_{AB}}{\partial u_{i\beta}^4}\right)_{eq}\right]_{r=r_{1A_2}} = \gamma_{1A} + \tfrac{1}{24}\frac{d^4\varphi_{AB}(r_{1A_2})}{dr_{1A_2}^4} + \frac{1}{4r_{1A_2}}\frac{d^3\varphi_{AB}(r_{1A_2})}{dr_{1A_2}^3} - \frac{1}{8r_{1A_2}^2}\frac{d^2\varphi_{AB}(r_{1A_2})}{dr_{1A_2}^2} + \frac{1}{8r_{1A_2}^3}\frac{d\varphi_{AB}(r_{1A_2})}{dr_{1A_2}}, \tag{14}$$

$$\gamma_{2A_2} = \gamma_{2A} + \tfrac{6}{48}\sum_i \left[\left(\frac{\partial^4 \varphi_{AB}}{\partial u_{i\alpha}^2 \partial u_{i\beta}^2}\right)_{eq}\right]_{r=r_{1A_2}} = \gamma_{2A} + \tfrac{1}{4}\frac{d^4\varphi_{AB}(r_{1A_2})}{dr_{1A_2}^4} - \frac{1}{4r_{1A_2}}\frac{d^3\varphi_{AB}(r_{1A_2})}{dr_{1A2}^3} + \frac{3}{2r_{1A_2}^2}\frac{d^2\varphi_{AB}(r_{1A_2})}{dr_{1A_2}^2} - \frac{3}{2r_{1A_2}^3}\frac{d\varphi_{AB}(r_{1A_2})}{dr_{1A_2}}, \tag{15}$$

where $r_{1A_2} = r_{01A_2} + y_{0B}(T), r_{01A_2}$ and $u_{0A_2}, y_{0B}(T)$ are the nearest neighbor distances between atom A_2 and the other atoms in the alloy, and is determined from the minimum condition of the cohesive energy in the displacement of atom B from the equilibrium position at temperature T. In Equations (6)–(15), $u_{0A}, k_A, \gamma_{1A}, \gamma_{2A}$ are the cohesive energy and the metal parameters for atom A in the clean metal A in the approximation of two

coordination spheres with the sphere center at the position of A and radii r_{1A} and r_{2A} and have the following forms [29,33]:

$$u_{0A} = 4\varphi_{AA}(r_{1A}) + 3\varphi_{AA}(r_{2A}),\ r_{2A} = \frac{2}{\sqrt{3}} r_{1A}, \tag{16}$$

$$k_A = \frac{4}{3}\frac{d^2\varphi_{AA}(r_{1A})}{dr_{1A}^2} + \frac{8}{3r_{1A}}\frac{d\varphi_{AA}(r_{1A})}{dr_{1A}} + \frac{d^2\varphi_{AA}(r_{2A})}{dr_{2A}^2} + \frac{2}{r_{2A}}\frac{d\varphi_{AA}(r_{2A})}{dr_{2A}}, \tag{17}$$

$$\gamma_A = 4(\gamma_{1A} + \gamma_{2A}). \tag{18}$$

$$\begin{gathered}\gamma_{1A} = \frac{1}{54}\frac{d^4\varphi_{AA}(r_{1A})}{dr_{1A}^4} + \frac{8}{9r_{1A}}\frac{d^3\varphi_{AA}(r_{1A})}{dr_{1A}^3} - \frac{20}{9r_{1A}^2}\frac{d^2\varphi_{AA}(r_{1A})}{dr_{1A}^2} + \frac{20}{9r_{1A}^3}\frac{d\varphi_{AA}(r_{1A})}{dr_{1A}} + \\ \frac{1}{24}\frac{d^4\varphi_{AA}(r_{2A})}{dr_{2A}^4} + \frac{1}{4r_{2A}^2}\frac{d^2\varphi_{AA}(r_{2A})}{dr_{2A}^2} - \frac{1}{4r_{2A}^3}\frac{d\varphi_{AA}(r_{2A})}{dr_{2A}},\end{gathered} \tag{19}$$

$$\begin{gathered}\gamma_{2A} = \frac{1}{54}\frac{d^4\varphi_{AA}(r_{1A})}{dr_{1A}^4} + \frac{5}{9r_{1A}}\frac{d^3\varphi_{AA}(r_{1A})}{dr_{1A}^3} + \frac{5}{18r_{1A}^2}\frac{d^2\varphi_{AA}(r_{1A})}{dr_{1A}^2} - \frac{5}{18r_{1A}^3}\frac{d\varphi_{AA}(r_{1A})}{dr_{1A}} + \\ \frac{1}{2r_{2A}}\frac{d^3\varphi_{AA}(r_{2A})}{dr_{2A}^3} - \frac{9}{8r_{2A}^2}\frac{d^2\varphi_{AA}(r_{2A})}{dr_{2A}^2} + \frac{9}{8r_{2A}^3}\frac{d\varphi_{AA}(r_{2A})}{dr_{2A}}.\end{gathered} \tag{20}$$

The equations of state for the BCC alloy AB at P and T, and at P and T = 0 K, respectively, are determined by the following relations [29,33]:

$$Pv = -r_1\left[\frac{1}{6}\frac{\partial u_0}{\partial r_1} + \theta x c t h x \frac{1}{2k}\frac{\partial k}{\partial r_1}\right], v = \frac{4r_1^3}{3\sqrt{3}}, \tag{21}$$

$$Pv = -r_1\left[\frac{1}{6}\frac{\partial u_0}{\partial r_1} + \frac{\hbar\omega_0}{4k}\frac{\partial k}{\partial r_1}\right]. \tag{22}$$

where r_1, v, $x = \frac{\hbar\omega}{2\theta}$, $\theta = k_{\mathrm{Bo}}T$, $\omega = \sqrt{\frac{k}{m}}$, k_{Bo} are the nearest neighbor distance between two atoms in the alloy, the volume of the cubic unit cell per atom, and the Boltzmann constant. If the form of the interaction potential between two atoms X (X = A, A_1, A_2, B) is known, from Equation (22) we can find the nearest neighbor distance between two $r_{01X}(P,0)$ and the alloy parameters $k_X(P,0)$, $\gamma_1(P,0)$, $\gamma_2(P,0)$, $\gamma(P,0)$ for atom X at T = 0 K and P. From that, we can determine the displacement $y_X(P,T)$ of atom X from the equilibrium position at T and P as follows [29,33]:

$$y_X(P,T) = \sqrt{\frac{2\gamma_X(P,0)(k_{\mathrm{Bo}}T)^2}{3k_X^3(P,0)}A_X(P,T)}, A_X(P,T) = a_{1X}(P,T) + \sum_{i=2}^{6}\left[\frac{\gamma_X(P,0)k_{\mathrm{Bo}}T}{k_X^2(P,0)}\right]^i a_{iX}(P,T),$$

$$Y_X(P,T) \equiv x_X(P,T)\coth x_X(P,T), x_X(P,T) = \frac{\hbar\omega_X(P,0)}{2k_{\mathrm{Bo}}T}, \omega_X(P,0) = \sqrt{\frac{k_X(P,0)}{m}},$$

$$\begin{gathered}a_{1X} = 1 + \tfrac{1}{2}Y_X, a_2 = \tfrac{13}{3} + \tfrac{47}{6}Y_X + \tfrac{22}{6}Y_X^2 + \tfrac{1}{2}Y_X^3, a_{3X} = -\left(\tfrac{25}{3} + \tfrac{121}{6}Y_X + \tfrac{50}{3}Y_X^2 + \tfrac{16}{3}Y_X^3 + \tfrac{1}{2}Y_X^4\right), \\ a_{4X} = \tfrac{43}{3} + \tfrac{93}{2}Y_X + \tfrac{169}{3}Y_X^2 + \tfrac{83}{3}Y_X^3 + \tfrac{22}{3}Y_X^4 + \tfrac{1}{2}Y_X^5, \\ a_{5X} = -\left(\tfrac{103}{3} + \tfrac{749}{6}Y_X + \tfrac{363}{2}Y_X^2 + \tfrac{391}{3}Y_X^3 + \tfrac{148}{3}Y_X^4 + \tfrac{53}{6}Y_X^5 + \tfrac{1}{2}Y_X^6\right), \\ a_{6X} = 65 + \tfrac{561}{2}Y_X + \tfrac{1489}{3}Y_X^2 + \tfrac{927}{2}Y_X^3 + \tfrac{733}{3}Y_X^4 + \tfrac{145}{2}Y_X^5 + \tfrac{31}{3}Y_X^6 + \tfrac{1}{2}Y_X^7.\end{gathered} \tag{23}$$

The nearest neighbor distance $r_{1X}(P,T)$ is given by the following relations [1–4]:

$$\begin{gathered}r_{1B}(P,T) = r_{01B}(P,0) + y_{A_1}(P,T), r_{1A}(P,T) = r_{01A}(P,0) + y_A(P,T), \\ r_{1A_1}(P,T) \approx r_{1B}(P,T), r_{1A_2}(P,T) = r_{01A_2}(P,0) + y_B(P,T).\end{gathered} \tag{24}$$

The mean nearest neighbor distance $\overline{r_{1A}(P,T)}$ between two atoms A in the alloy is derived from the following expressions [1–4]:

$$\begin{gathered}\overline{r_{1A}(P,T)} = \overline{r_{01A}(P,0)} + \overline{y(P,T)},\\ \overline{r_{01A}(P,0)} = (1-c_B)r_{01A}(P,0) + c_B r'_{01A}(P,0), r'_{01A}(P,0) = \sqrt{3}r_{01B}(P,0),\\ \overline{y(P,T)} = (1-7c_B)y_A(P,T) + c_B y_B(P,T) + 2c_B y_{A_1}(P,T) + 4c_B y_{A_2}(P,T),\end{gathered} \tag{25}$$

where $r_{01A}(P,0)$, $r'_{01A}(P,0)$, $\overline{r_{1A}(P,T)}$, $\overline{r_{01A}(P,0)}$ and c_B are the mean nearest neighbor distances between two atoms A in the clean metal A at pressure P and temperature 0 K; the region containing the interstitial atom C of the alloy at P and T = 0 K, and the concentration of the interstitial atoms B and nearest neighbor distance between two atoms A in the alloy at P and T and at P and T = 0 K. The Helmholtz free energy of the BCC perfect interstitial alloy AB with the condition $c_B << c_A$ (c_A, c_B, respectively, are the concentrations of atoms A and B) can be calculated with the following relations [1–4]:

$$\begin{gathered}\psi_{AB} = (1-7c_B)\psi_A + c_B\psi_B + 2c_B\psi_{A_1} + 4c_B\psi_{A_2} - TS_C,\\ \psi_X \approx U_{0X} + \psi_{0X} + 3N\left\{\frac{\theta^2}{k_X^2}\left[\gamma_{2X}Y_X^2 - \frac{2\gamma_{1X}}{3}\left(1+\frac{Y_X}{2}\right)\right] + \right.\\ \left.\frac{2\theta^3}{k_X^4}\left[\frac{4}{3}\gamma_{2X}Y_X\left(1+\frac{Y_X}{2}\right) - 2\left[\gamma_{1X}^2 + 2\gamma_{1X}\gamma_{2X}\right]\left(1+\frac{Y_X}{2}\right)(1+Y_X)\right]\right\},\\ \psi_{0X} = 3N\theta\left[x_X + \ln\left(1-e^{-2x_X}\right)\right], Y_X \equiv x_X \coth x_X,\end{gathered} \tag{26}$$

where N is the number of atoms in the alloy, ψ_X is the Helmholtz free energy of atom X in the clean material X, and S_C is the configurational entropy of the interstitial alloy AB.

The concentrations of atoms A, A_1, A_2 and B are determined by the following relations:

$$c_A = 1 - 7c_B, c_{A_1} = 2c_B, c_{A_2} = 4c_B, c_B << c_A. \tag{27}$$

From the condition of absolute stability limit expressed as:

$$\left(\frac{\partial P}{\partial v_{AB}}\right)_{T=T_S} = 0 \text{ or } \left(\frac{\partial P}{\partial a_{AB}}\right)_{T=T_S} = 0 \tag{28}$$

and from the equation of state for the interstitial alloy AB expressed as:

$$P = -\frac{a_{AB}}{v_{AB}}\sum_X c_X \frac{\partial u_{0X}}{\partial r_{1X}} + \frac{3\gamma_G^T k_{\mathrm{Bo}} T}{v_{AB}}, \tag{29}$$

the absolute stability temperature for the crystalline state can be derived in the following expression [3,4,29,32,33]:

$$T_S = \frac{2Pv_{AB} + \frac{a_{AB}^2}{6}\sum_X c_X \frac{\partial^2 u_{0X}}{\partial r_{1X}^2} - \frac{\hbar a_{AB}^2}{4}\sum_X \frac{c_X\omega_X}{k_X}\left[\frac{1}{2k_X}\left(\frac{\partial k_X}{\partial r_{1X}}\right)^2 - \frac{\partial^2 k_X}{\partial r_{1X}^2}\right]}{\frac{a_{AB}^2 k_{\mathrm{Bo}}}{4}\sum_X \frac{c_X}{k_X^2}\left(\frac{\partial k_X}{\partial r_{1X}}\right)^2}, \tag{30}$$

where $a_{AB} \equiv \overline{r_{1A}(P,T)}$, $v_{AB} = \frac{4a_{AB}^3}{3\sqrt{3}}$ and $\gamma_G^T = -\frac{a_{AB}}{6}\sum_X \frac{c_X}{k_X}\frac{\partial k_X}{\partial r_{1X}} Y_X, Y_X \equiv x_X \coth x_X$. γ_G^T are the Gruneisen parameters of the alloy. The right side of Equation (30) must be determined at T_S. By solving Equation (30) the value of T_S can be obtained.

The melting temperature T_m is derived from the absolute stability temperature T_S by the following relation [3,4,29,32,33]:

$$T_m \approx T_S + \frac{a_m - a_S}{k_{Bo}\gamma_G^S}\left\{\frac{Pv_S}{a_S} + \sum_X \frac{c_X}{18}\left[\left(\frac{\partial u_{0X}}{\partial r_{1X}}\right)_{T=T_S} + a_S\left(\frac{\partial^2 u_{0X}}{\partial r_{1X}^2}\right)_{T=T_S}\right]\right\}, \tag{31}$$

where $a_m = a_{AB}(T_m)$, $a_S = a_{AB}(T_S)$, $v_S = v_{AB}(T_S)$ and $\gamma_G^S = \gamma_G^T(T_S)$. Here, approximately γ_G^S is constant in the range of temperature from T_S to T_m.

Temperature $T_S(0)$ at zero pressure has the following relation [3,4]:

$$T_S(0) = \frac{a_{AB}}{18\gamma_G^T k_{Bo}} \sum_X c_X \frac{\partial u_{0X}}{\partial r_{1X}}, \tag{32}$$

where a_{AB}, $\frac{\partial u_{0X}}{\partial r_{1X}}$, γ_G^T are determined at $T_S(0)$.

Temperature T_S at pressure P can be calculated with the following relation [3,4]:

$$T_S \approx T_S(0) + \frac{v_{AB} P}{3k_{Bo}\left(\gamma_G^T\right)^2} \left(\frac{\partial \gamma_G^T}{\partial T}\right)_{a_{AB}} T_S. \tag{33}$$

Here, v_{AB}, γ_G^T, $\frac{\partial \gamma_G^T}{\partial T}$ are calculated at T_S. Approximately, the $T_m \approx T_S$. Equation (33) can be solved by the approximate iteration method applied at low pressure.

In the case of high pressure, temperature T_m at pressure P is calculated by the following relation [3,4]:

$$T_m(P) = \frac{T_m(0) B_0^{1/B_0'}}{G(0)} \frac{G(P)}{\left(B_0 + B_0' P\right)^{1/B_0'}}, \tag{34}$$

where $T_m(P)$, $T_m(0)$, G and B_T are the melting T at P and at zero P, respectively; the bulk modulus and the isothermal elastic modulus are calculated by the following relations [1–4,29,33]:

$$\begin{gathered}
G = \frac{E}{2(1+\nu)}, \nu \equiv \nu_{AB} \cong \nu_A, B_0 \equiv B_T(0), B_0' = \left(\frac{dB_T}{dP}\right)_{P=0}, \\
B_T(P) = \frac{1}{\chi_T(P)} = \frac{2P + \frac{a_{AB}^2}{3V_{AB}}\left(\frac{\partial^2 \psi_{AB}}{\partial a_{AB}^2}\right)_T}{3\left(\frac{a_{AB}}{a_{0AB}}\right)^3}, \left(\frac{\partial^2 \psi_{AB}}{\partial a_{AB}^2}\right)_T \approx \sum_X c_X \left(\frac{\partial^2 \psi_X}{\partial r_{1X}^2}\right)_T, \\
\frac{1}{3N}\left(\frac{\partial^2 \psi_X}{\partial r_{1X}^2}\right)_T = \frac{1}{6}\frac{\partial^2 u_{0X}}{\partial r_{1X}^2} + \theta\left[\frac{Y_X}{2k_X}\frac{\partial^2 k_X}{\partial r_{1X}^2} - \frac{1}{4k_X^2}\left(\frac{\partial k_X}{\partial r_{1X}}\right)^2 \left(Y_X + Z_X^2\right)\right], Z_X \equiv \frac{x_X}{\sinh x_X}, \\
E = \frac{1}{\pi r_{1A} A_{1A}}\left(1 - 7c_B + c_B \frac{\frac{\partial^2 \psi_B}{\partial \varepsilon^2} + 2\frac{\partial^2 \psi_{A_1}}{\partial \varepsilon^2} + 4\frac{\partial^2 \psi_{A_2}}{\partial \varepsilon^2}}{\frac{\partial^2 \psi_A}{\partial \varepsilon^2}}\right), \\
A_{1A} = \frac{1}{k_A}\left[1 + \frac{2\gamma_A^2 \theta^2}{k_A^4}\left(1 + \frac{1}{2}Y_A\right)\left(1 + Y_A\right)\right], \\
\frac{\partial^2 \psi_X}{\partial \varepsilon^2} = \left\{2\frac{\partial^2 u_{0X}}{\partial r_{1X}^2} + 3\frac{\hbar \omega_X}{k_X}\left[\frac{\partial^2 k_X}{\partial r_{1X}^2} - \frac{1}{2k_X}\left(\frac{\partial k_X}{\partial r_{1X}}\right)^2\right]\right\} r_{01X}^2 + \left(\frac{\partial u_{0X}}{\partial r_{1X}} + \frac{3\theta Y_X}{k_X}\frac{\partial k_X}{\partial a_X}\right) r_{01X},
\end{gathered} \tag{35}$$

where ε is the strain of the alloy, and ν_{AB}, ν_A are the Poisson ratios of alloy AB and the main metal A, respectively.

The equilibrium vacancy concentration n_v of the alloy is determined from the minimum condition of the real Gibbs thermodynamic potential G_{AB}^R of the defective alloy AB, and has the following relation form:

$$n_v = \frac{n}{N} = \exp\left(-\frac{g_{vAB}^f}{k_{Bo} T}\right), \tag{36}$$

where n and g_{vAB}^f are the numbers of vacancies in the alloy and the change in the Gibbs thermodynamic potential when a vacancy is formulated, and is determined from the distribution of atomic concentrations c_X as follows:

$$g_{vAB}^f = \sum_X c_X g_{vX}^f, \tag{37}$$

$$g_{vX}^f = -\frac{u_{0X}}{2} + (B_X - 1)\psi_X + P\Delta v_X, \tag{38}$$

where $B_X \approx 1 + \frac{u_{0X}}{\psi_X}$. Therefore, $g^f_{vX} \approx -\frac{u_{0X}}{4}$ and according to ref. [34]:

$$n_v = \exp\left(\frac{\sum\limits_X c_X u_{0X}}{4k_{\mathrm{Bo}}T}\right). \tag{39}$$

At constant P and constant interstitial atom concentration, the melting temperature T_m^R of a defective crystal is the function of the equilibrium vacancy concentration n_v. Approximately, the following relations can be applied [2,34]:

$$\begin{gathered}
T_m^R(P) \approx T_m(P) + \left(\frac{\partial T_m}{\partial n_v}\right) n_v = T_m(P) + \frac{T_m^2(P)}{T_m(P)\frac{\partial g^f_{vAB}}{\partial(k_{\mathrm{Bo}}T)} - \frac{g^f_{vAB}}{k_{\mathrm{Bo}}}}, \\
\frac{\partial g^f_{vAB}}{\partial(k_{\mathrm{Bo}}T)} = -\frac{a_{0AB}\alpha_T}{4k_{\mathrm{Bo}}}\sum c_X \frac{\partial u_{0X}}{\partial r_{1X}}, \\
\alpha_T = \frac{k_{\mathrm{Bo}}}{a_{0AB}}\frac{da_{AB}}{d\theta} = -\frac{k_{\mathrm{Bo}}\chi_T}{3}\left(\frac{a_{0AB}}{a_{AB}}\right)^2 \frac{a_{AB}}{v_{AB}}\frac{1}{3N}\frac{\partial^2\psi_{AB}}{\partial\theta\partial a_{AB}}, \frac{\partial^2\psi_{AB}}{\partial\theta\partial a_{AB}} \approx \sum_X c_X \frac{\partial^2\psi_X}{\partial\theta\partial r_{1X}}, \\
\frac{1}{3N}\frac{\partial^2\psi_X}{\partial\theta\partial a_X} = \frac{1}{2k_X}\frac{\partial k_X}{\partial a_X}Z_X^2 + \frac{2\theta}{k_X^2}\left[\frac{\gamma_{1X}}{3k_X}\frac{\partial k_X}{\partial a_X}\left(2 + Y_X Z_X^2\right) - \frac{1}{6}\frac{\partial\gamma_{1X}}{\partial a_X}\left(4 + Y_X + Z_X^2\right) - \right. \\
\left.\left(\frac{2\gamma_{2X}}{k_X}\frac{\partial k_X}{\partial a_X} - \frac{\partial\gamma_{2X}}{\partial a_X}\right) Y_X Z_X^2\right.
\end{gathered} \tag{40}$$

where α_{TX}, α_T, respectively, are the thermal expansion coefficients of atom X in alloy AB.

The jumping of volume at melting point for the alloy can be found from the following expression [35]:

$$\Delta v_m = \frac{\varepsilon\theta a_{AB}^3}{\sqrt{2}k\langle u\rangle^2}\left(1 + \frac{6\gamma^2\theta^2}{k^4}\right), \tag{41}$$

where ε is a constant depending on the nature of the alloy and we take the value 0.01 as for metal [36], and $\langle u\rangle = \overline{y} = \sum\limits_X c_X y_X$ is the mean displacement of the main metal atom A from the equilibrium position as in Equation (25). In order to determine the jumping of volume Δv_m at pressure P and temperature T, it is necessary to determine a_{AB}, $\langle u\rangle$ at pressure P and temperature T. The alloy parameters k, γ are determined with respect to a_{AB} at pressure P and temperature T.

After finding the melting temperature T_m and the melting T_m (P), we can calculate the slope of this curve, and the derivative $\frac{\partial T_m}{\partial P}$. If T_m, $\frac{\partial T_m}{\partial P}$ and Δv_m, are known, the jumping of enthalpy at melting point from the Clausius–Clapeyron equation can be derived according to the following relation:

$$\Delta H_m = \frac{T_m \Delta v_m}{\frac{\partial T_m}{\partial P}} \tag{42}$$

and the jumping of entropy at melting point:

$$\Delta S_m = \frac{\Delta H_m}{T_m}. \tag{43}$$

Firstly, we find the isothermal compressibility χ_T of the BCC interstitial alloy AB according to Equation (35) and the thermal expansion coefficient α_T of the alloy according to Equation (40). The specific capacity at a constant volume of the alloy is given by the following relations [2,29,33]:

$$\begin{gathered}
C_{VAB} = \sum_X c_X C_{VX}, \\
C_{VX} = 3Nk_{\mathrm{Bo}}\left\{Z_X^2 + \frac{2\theta}{k_X^2}\left(2\gamma_{2X} + \frac{\gamma_{1X}}{3}\right) Y_X Z_X^2 + \frac{\gamma_{1X}}{3}\left(1 + Z_X^2\right) - \gamma_{2X}\left(Z_X^4 + Y_X^2 Z_X^2\right)\right]\right\}.
\end{gathered} \tag{44}$$

The Gruneisen parameter of the alloy has the following relation [29,33]:

$$\gamma_{\mathrm{G}} = \frac{3\alpha V}{\chi_T C_V V}. \tag{45}$$

Then, from the mean nearest neighbor distance a_{AB} the quantities V, χ_T, α_T, C_V and γ_G at pressure P and temperature T can be determined. For the BCC lattice, the following relation is known:

$$\frac{V(P,T)}{V_0(0,T)} = \left[\frac{a_{AB}(P,T)}{a_{0AB}(0,T)}\right]^3. \tag{46}$$

Graf et al. [37] proposed the following expression for the Gruneisen parameter:

$$\gamma_G = \gamma_{G0}\left(\frac{V}{V_0}\right)^q, \tag{47}$$

where $\gamma_G = \gamma_G(P,T)$, $\gamma_{G0} = \gamma_G(0,T)$ and q are material constants and $q > 0$. Therefore, by using the SMM, γ_G, γ_{G0}, $\frac{V}{V_0}$ can be calculated from a_{AB}, and by using Equation (49) the value of q can be calculated.

According to the Debye model, the Gruneisen parameter is defined as follows:

$$\gamma_G = -\frac{\partial \ln \omega_D}{\partial \ln V} = -\frac{\partial \ln \frac{k_{Bo}T_D}{\hbar}}{\partial \ln V}, \tag{48}$$

where ω_D is the Debye frequency and T_D is the Debye temperature.

By substituting the Gruneisen parameter from Equation (47) into Equation (48) and taking the integration, we derived the dependence of the Debye temperature $T_D(P)$ at P on the Debye temperature T_{D0}, and the Gruneisen parameter γ_{G0} at zero P, as well as the volume ratio $\frac{V}{V_0}$ [7]:

$$T_D(P) = T_{D0}\exp\left\{-\frac{\gamma_{G0}}{q}\left[\left(\frac{V}{V_0}\right)^q - 1\right]\right\}. \tag{49}$$

The Debye temperature T_{D0} of the alloy at zero pressure is given by the following relation:

$$T_{D0} = \frac{\hbar\omega_D(0,T)}{k_{Bo}}. \tag{50}$$

The Debye frequency $\omega_D(0,T)$ at zero pressure and temperature T is related to the Einstein frequency $\omega_E(0,T)$ at zero pressure and temperature T by the following relation [38]:

$$\omega_D(0,T) \approx \frac{4}{3}\omega_E(0,T) \approx \frac{4}{3}\sqrt{\frac{k(0,T)}{m}}, \tag{51}$$

where $k(0,T)$ is the harmonic parameter of the alloy at zero pressure and temperature T. Therefore, it can be obtained through the following expression:

$$T_{D0} = \frac{4\hbar}{3k_{Bo}}\sqrt{\frac{k(0,T)}{m}}. \tag{52}$$

Equations (1)–(40) are used in our previous papers [1–9] on elastic, thermodynamic and melting properties of metals and interstitial alloys. Equations (41)–(52) only are used to study the jumps of volume, enthalpy and entropy, and the Debye temperature of metals. In this study, for the first time, we apply Equations (41)–(52) to study the jumps of volume, enthalpy and entropy, and the Debye temperature of the BCC interstitial alloy AB.

2.2. Numerical Results and Discussions for Alloy WSi

In order to study alloy WSi, we applied the Mie–Lennard-Jones (MLJ) pair interaction potential as follows [39]:

$$\varphi(r) = \frac{D}{n-m}\left[m\left(\frac{r_0}{r}\right)^n - n\left(\frac{r_0}{r}\right)^m\right], \tag{53}$$

where D, r_0, m and n are the depths of potential well corresponding to the equilibrium distance—they are determined empirically. Then, the potential parameters for the interaction W–Si are determined by the following relations [28]:

$$D_{\mathrm{W-Si}} = \sqrt{D_{\mathrm{W-W}} D_{\mathrm{Si-Si}}}, r_{0\mathrm{W-Si}} = \frac{1}{2}(r_{0\mathrm{W-W}} + r_{0\mathrm{Si-Si}}). \quad (54)$$

We find $n_{\text{W-Si}}$, $m_{\text{W-Si}}$ by fitting the experimental data and the theoretical result for the Young modulus of the interstitial alloy WSi at room temperature. The Mie–Lennard-Jones potential's parameters for the interactions of W–W and Si–Si are given in Table 1.

Table 1. Mie–Lennard-Jones potential's parameters for the interactions W–W and Si–Si.

Interaction	D (10^{-16} erg)	r_0 (10^{-10} m)	m	n
W–W [31]	15,564.744	2.7365	6.5	10.5
Si–Si [31]	45,128.34	2.2950	6	12

Our computed results are summarised from Tables 2–9 and are illustrated in Figures 1–9. We calculated the silicon concentration and pressure of the volume, the isothermal compressibility, the Gruneisen parameter and the Debye temperature, the thermal expansion coefficient, the specific heat at constant volume in Tables 2–7 and in Figures 1–6. According to our obtained results, for WSi at the same temperature and silicon concentration when pressure increases, the volume, the isothermal compressibility, the thermal expansion coefficient, the Gruneisen parameter decreases, the Debye temperature increases, and the specific heat at constant volume. For WSi at the same temperature and pressure when the silicon concentration increases, the volume, the specific heat at constant volume, the Gruneisen parameter increases, the thermal expansion coefficient, the Debye temperature decreases and the isothermal compressibility.

Table 2. Si concentration and pressure dependence of volume $V\ (10^{-29}\mathrm{m}^3)$ for WSi at T = 300 K.

		P = 0 GPa	P = 10 GPa	P = 30 GPa	P = 50 GPa	P = 70 GPa
$V\ (10^{-29}\ \mathrm{m}^3)$	$c_{\mathrm{Si}} = 0\%$	1.442	1.412	1.372	1.339	1.311
	$c_{\mathrm{Si}} = 1\%$	1.474	1.439	1.396	1.362	1.333
	$c_{\mathrm{Si}} = 3\%$	1.537	1.496	1.446	1.408	1.377
	$c_{\mathrm{Si}} = 5\%$	1.603	1.554	1.498	1.456	1.422

Table 3. Si concentration and pressure dependence of isothermal compressibility $\chi_T\ \left(10^{-12}\mathrm{Pa}^{-1}\right)$ for WSi at T = 300 K.

		P = 0 GPa	P = 10 GPa	P = 30 GPa	P = 50 GPa	P = 70 GPa
χ_T $\left(10^{-12}\mathrm{Pa}^{-1}\right)$	$c_{\mathrm{Si}} = 0\%$	1.666	1.501	1.271	1.107	0.984
	$c_{\mathrm{Si}} = 1\%$	1.845	1.647	1.375	1.186	1.045
	$c_{\mathrm{Si}} = 3\%$	2.338	2.035	1.639	1.378	1.192
	$c_{\mathrm{Si}} = 5\%$	3.160	2.643	2.017	1.638	1.381

Table 4. Si concentration and pressure dependence of thermal expansion coefficient $\alpha_{\mathrm{T}}\left(10^{-6}\ \mathrm{K}^{-1}\right)$ for WSi at T = 300 K.

		P = 0 GPa	P = 10 GPa	P = 30 GPa	P = 50 GPa	P = 70 GPa
-	$c_{\mathrm{Si}} = 0\%$	3.320	3.025	2.583	2.264	2.021
α_T	$c_{\mathrm{Si}} = 1\%$	3.893	3.39	2.819	2.435	2.151
$\left(10^{-6}\mathrm{K}^{-1}\right)$	$c_{\mathrm{Si}} = 3\%$	5.456	4.356	3.414	2.851	2.459
-	$c_{\mathrm{Si}} = 5\%$	8.040	5.859	4.264	3.412	2.856

Table 5. Si concentration and pressure dependence of specific capacity at constant volume C_V(J/mol.K) for WSi at T = 300 K.

		P = 0 GPa	**P = 10 GPa**	**P = 30 GPa**	**P = 50 GPa**	**P = 70 GPa**
C_V (J/mol.K)	$c_{Si} = 0\%$	23.402	23.294	23.089	22.896	22.713
	$c_{Si} = 1\%$	23.544	23.294	22.982	22.728	22.499
	$c_{Si} = 3\%$	23.826	23.295	22.768	22.389	22.071
	$c_{Si} = 5\%$	24.109	23.295	22.554	22.051	21.642

Table 6. Si concentration and pressure dependence of the Gruneisen parameter γ_G. for WSi at T = 300 K.

		P = 0 GPa	**P = 10 GPa**	**P = 30 GPa**	**P = 50 GPa**	**P = 70 GPa**
γ_G	$c_{Si} = 0\%$	2.218	2.207	2.181	2.160	2.142
	$c_{Si} = 1\%$	2.386	2.298	2.249	2.222	2.202
	$c_{Si} = 3\%$	2.721	2.483	2.391	2.351	2.325
	$c_{Si} = 5\%$	3.057	2.673	2.536	2.485	2.454

Table 7. Si concentration and pressure dependence of Debye temperature T_D for WSi at T = 300 K.

		P = 0 GPa	**P = 10 GPa**	**P = 30 GPa**	**P = 50 GPa**	**P = 70 GPa**
T_D(K)	$c_{Si} = 0\%$	362.73	398.07	450.56	498.53	544.14
	$c_{Si} = 1\%$	330.05	365.98	418.01	464.84	509.11
	$c_{Si} = 3\%$	270.57	307.84	358.63	403.04	444.60
	$c_{Si} = 5\%$	219.02	257.24	306.32	348.15	386.97

Table 8. Si concentration and pressure dependence of volume jumping Δv_m $\left(10^{-30}\mathrm{m}^3\right)$ for WSi at T = 300 K.

		P = 0 GPa	**P = 10 GPa**	**P = 30 GPa**	**P = 50 GPa**	**P = 70 GPa**
Δv_m $\left(10^{-30}\mathrm{m}^3\right)$	$c_{Si} = 0$	2.43	2.16	1.84	1.62	1.44
	$c_{Si} = 1\%$	2.74	2.41	2.03	1.77	1.58
	$c_{Si} = 3\%$	3.49	2.99	2.47	2.13	1.88
	$c_{Si} = 5\%$	4.45	3.71	3.00	2.56	2.24

Table 9. Jumping of volume, and enthalpy and entropy at melting point (using the melting curve calculated by the SMM for the defective model).

P (GPa)	**0**	**30**	**50**	**70**
T_m (K)	3387.5	4312.5	4825	5312.5
$\frac{dT_m}{dP}$ (K/GPa)	34.6	27.5	25	25
$\Delta v_m\left(10^{-30}\mathrm{m}^3\right)$	2.743	2.301	1.772	1.576
ΔH_m (meV)	268.55	360.84	341.996	334.9
ΔS_m (k_B)	0.079	0.084	0.071	0.063

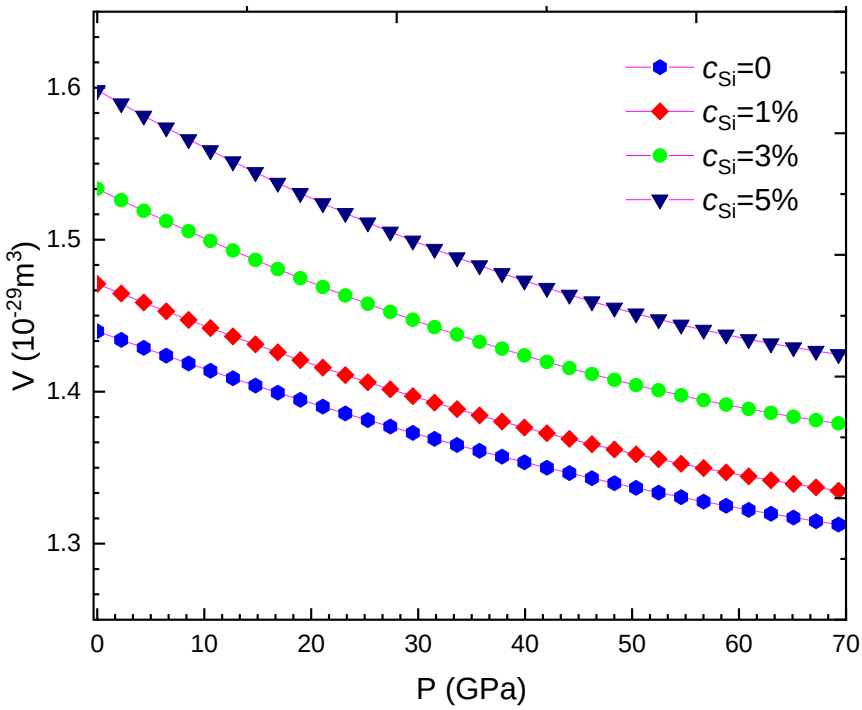

Figure 1. For WSi at T = 300 K.

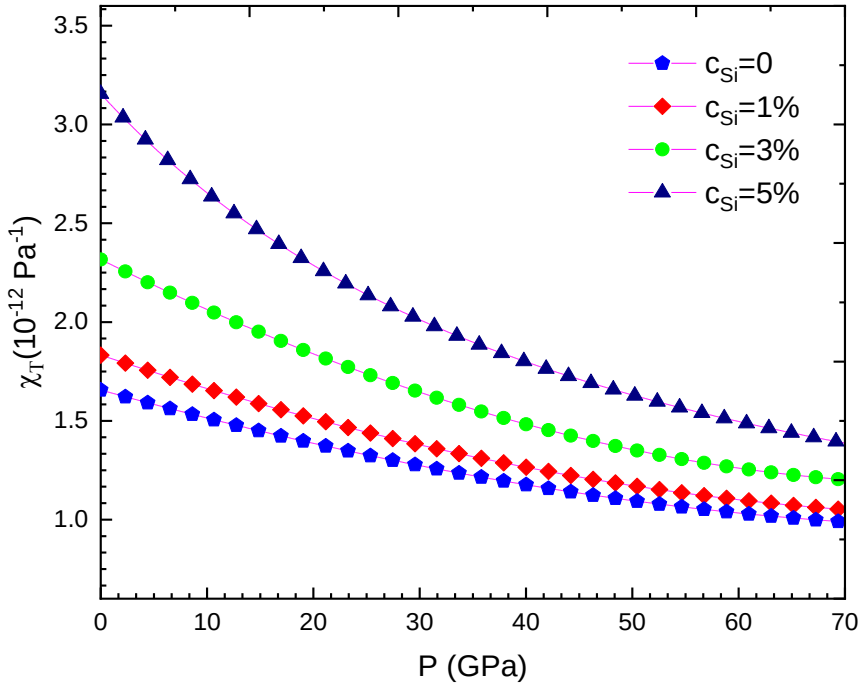

Figure 2. For WSi at T = 300 K.

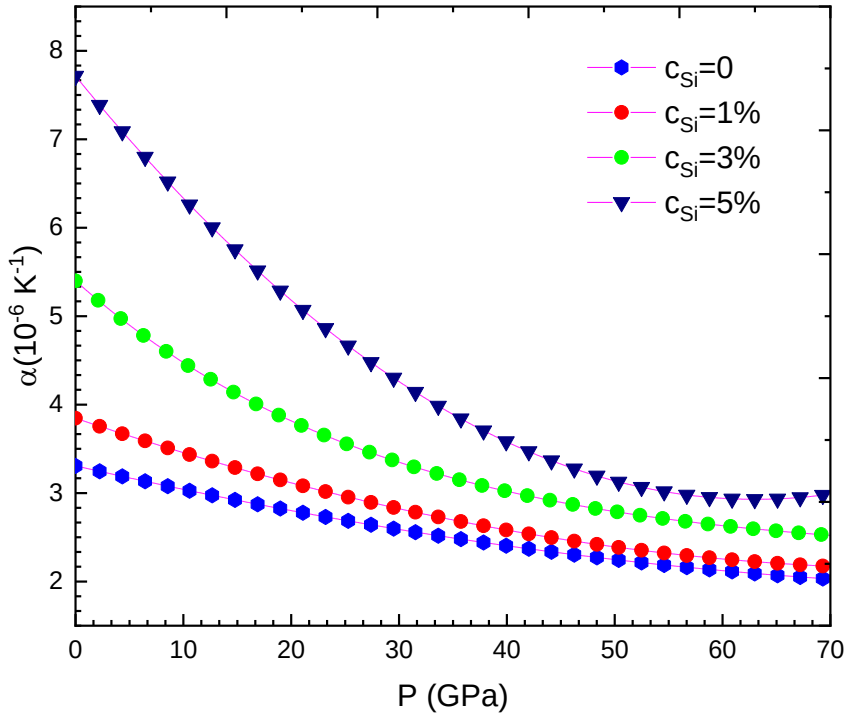

Figure 3. For WSi at T = 300 K.

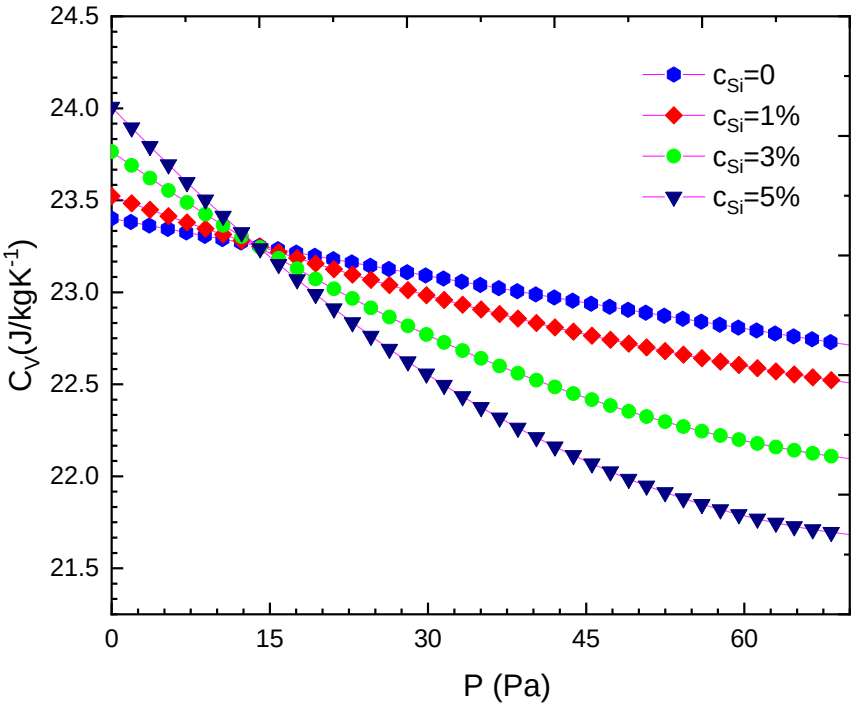

Figure 4. For WSi at T = 300 K.

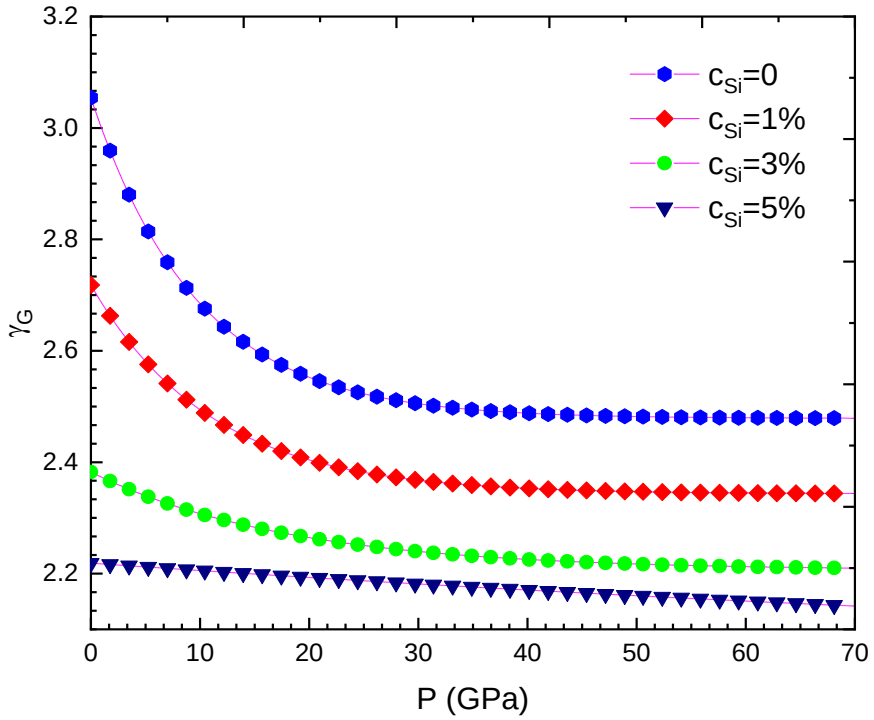

Figure 5. For WSi at T = 300 K.

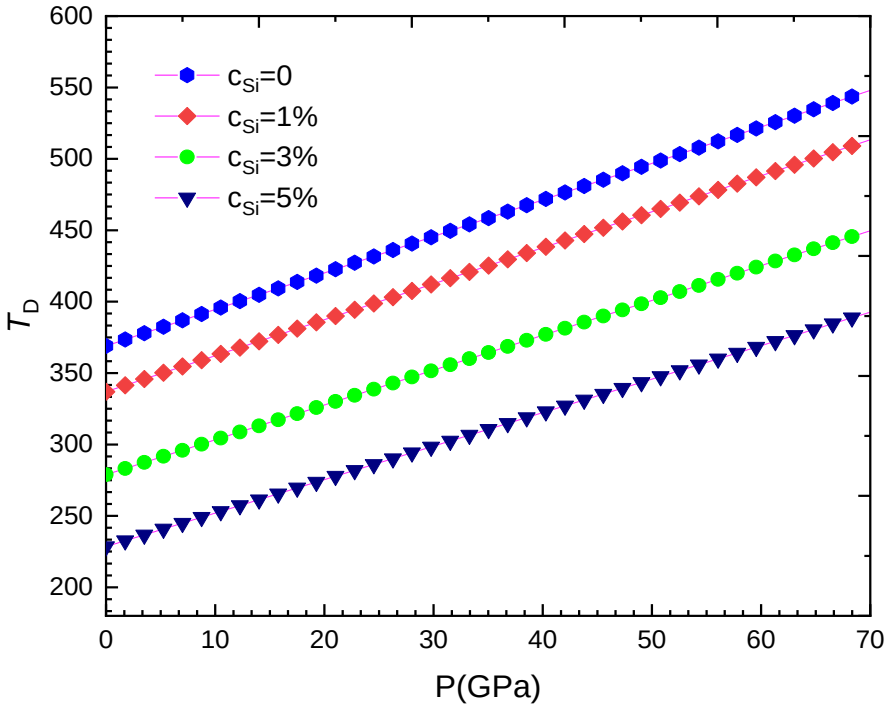

Figure 6. For WSi at T = 300 K.

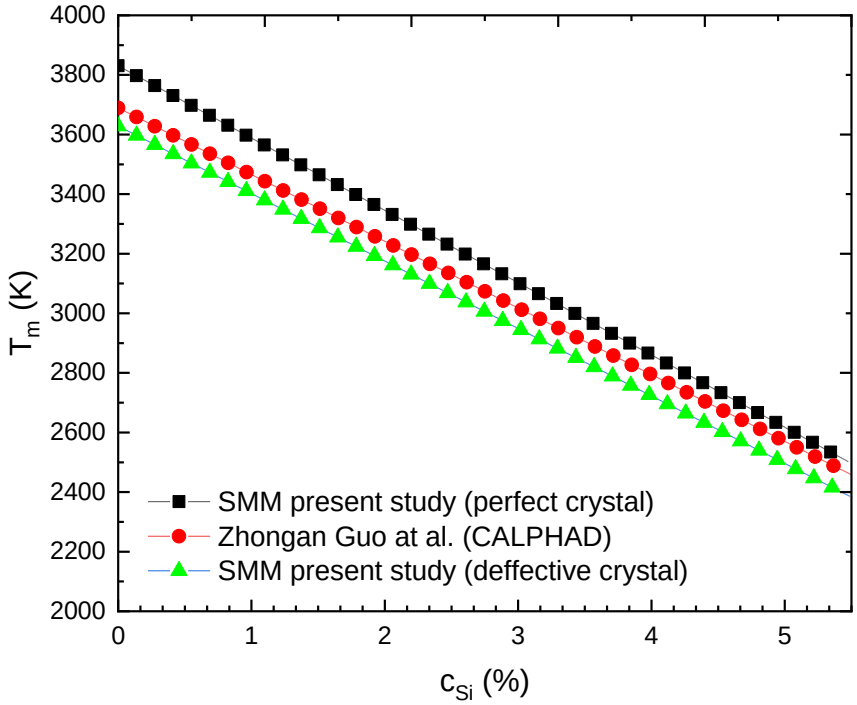

Figure 7. For WSi at $P = 0$ obtained from the SMM for the perfect model [3], the SMM for the defective model [3] and CALPHAD [40].

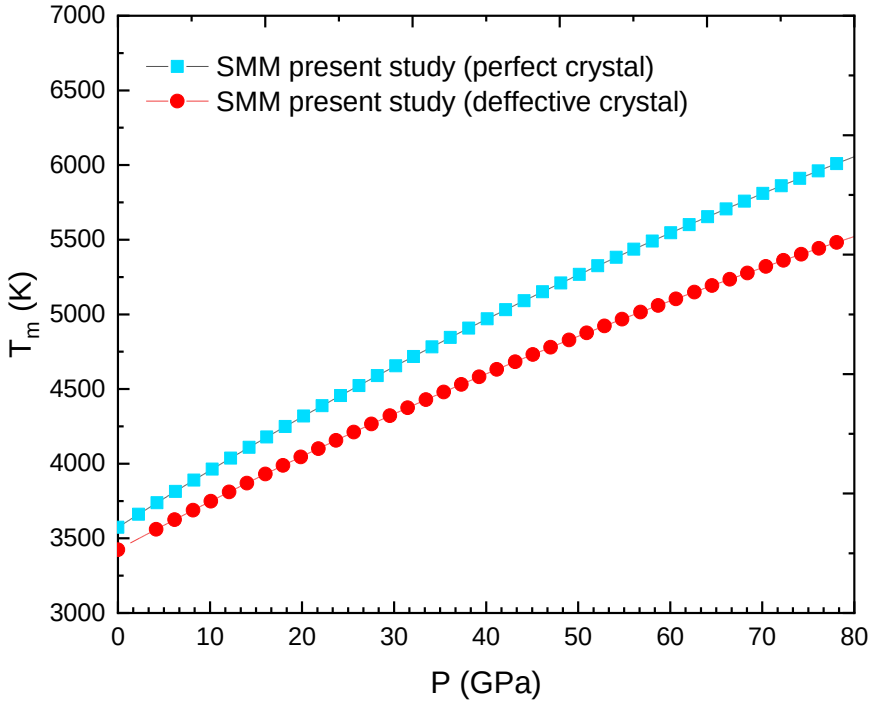

Figure 8. $T_m(P)$ for WSi at $c_{Si} = 1\%$ obtained from the SMM for the perfect model and the SMM for the defective model [3].

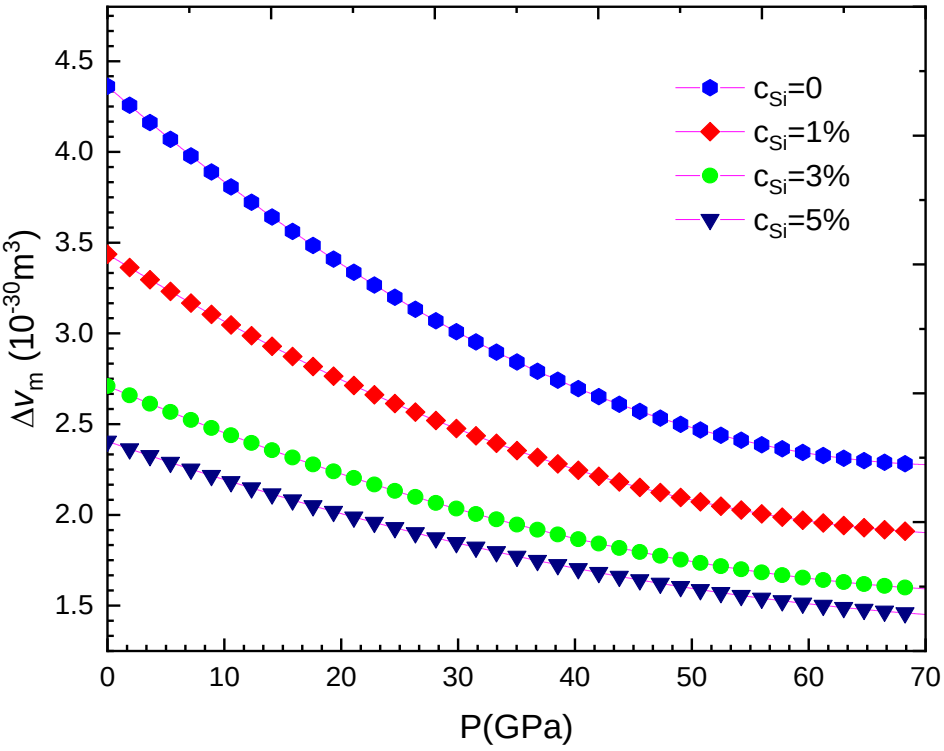

Figure 9. For WSi at T = 300 K.

According to Figure 7 [3], when c_{Si} increases from 0 to 5.5%, the T_m of WSi decreases (from 3810 to T = 2459 K) from the SMM for the perfect model, (from T = 3609 K to T = 2366 K) from the SMM for the defective model and from T = 3695 K to T = 2460 K from CALPHAD [40]. The melting slope $\frac{dT_m}{dc_{Si}}$ for WSi at zero pressure is 245.6 K/% from the SMM for the perfect alloy, 226 K/% from the SMM for the defective alloy and 224.5K/% from CALPHAD [40]. The SMM calculations for the melting slope of the defective alloy are in good agreement with the CALPHAD calculations.

Figure 8 shows the melting curve of WSi at c_{Si} = 1% obtained from the SMM for the perfect model and the SMM for the defective model [3]. In the range of pressure from P = 0 GPa to P = 80 GPa, the T_m of the perfect $W_{0.99}Si_{0.01}$ increases from T = 3564 K to T = 6088 K and the T_m of the defective $W_{0.99}Si_{0.01}$ increases from T = 3383 K to T = 5534 K.

3. Conclusions

The analytic expressions for structural and thermodynamic quantities such as the alloy parameters, the mean nearest neighbor distance, the melting temperature, the Helmholtz free energy, the equilibrium vacancy concentration, the cohesive energy, enthalpy and entropy, the isothermal compressibility, the limiting temperature of absolute stability for the crystalline state, the thermal expansion coefficient, the jumps of volume, the heat capacity at constant volume, the Gruneisen parameter and the Debye temperature for the defective and perfect binary interstitial alloy with a BCC structure are derived by combining the limiting condition of the absolute stability of the crystalline state with the statistical moment method, the Clapeyron–Clausius equation, the Debye model and the Gruneisen equation. Our numerical calculations of the melting curve and the relation are carried out for alloy WSi under a pressure of up to P = 80 GPa. Our calculated melting curve and relation between the melting temperature and the silicon concentration for WSi are in good agreement with other calculations. Our calculations for the melting curve, the jumping of volume, enthalpy and entropy, and the Debye temperature for WSi predict and orient experimental results in the future.

Author Contributions: H.N.Q.: conceptualization, methodology, validation, investigation, writing—original draft preparation, data curation. H.N.D.: writing—original draft preparation. D.N.T.: writing—original draft preparation, writing—review and editing. V.C.L.: writing—original draft preparation. Ş.Ţ.: writing—review and editing. All authors have read and agreed to the published version of the manuscript.

Funding: This research received no external funding.

Data Availability Statement: The data that support the findings of this study are available from the corresponding author upon reasonable request.

Conflicts of Interest: The authors declare no conflict of interest.

References

1. Hoc, N.Q.; Tinh, B.D.; Hien, N.D. Elastic moduli and elastic constants of interstitial alloy AuCuSi with FCC structure under pressure. *High Temp. Mater. Proc.* **2019**, *38*, 264–272. [CrossRef]
2. Tinh, B.D.; Hoc, N.Q.; Vinh, D.Q.; Cuong, T.D.; Hien, N.D. Thermodynamic and elastic properties of interstitial alloy FeC with BCC structure at zero pressure. *Adv. Mater. Sci. Eng.* **2018**, 5251741. [CrossRef]
3. Hoc, N.Q.; Cuong, T.D.; Tinh, B.D.; Viet, L.H. Study on the melting of defective interstitial alloys TaSi and WSi with BCC structure. *J. Korean Phys. Soc.* **2019**, *71*, 801–805. [CrossRef]
4. Tuyen, L.T.C.; Học, N.Q.; Tinh, B.D.; Vinh, D.Q.; Cuong, T.D. Study on the melting of interstitial alloys FeH and FeC with BCC structure under pressure. *Chin. J. Phys.* **2019**, *59*, 1–9. [CrossRef]
5. Cuong, T.D.; Hoc, N.Q.; Phan, A.D. Application of the statistical moment method to melting properties of ternary alloys with FCC structure. *J. Appl. Phys.* **2019**, *125*, 215306. [CrossRef]
6. Hoc, N.Q.; Viet, L.H.; Dung, N.T. On the melting of defective FCC interstitial alloy FeC under pressure up to 100 GPa. *J. Electron. Mater.* **2020**, *49*, 910–916. [CrossRef]
7. Hoc, N.Q.; Tinh, B.D.; Hien, N.D. Influence of temperature and pressure on the electrical resistivity of gold and copper up to 1350K and 100GPa. *Mater. Res. Bull.* **2020**, *128*, 110874. [CrossRef]
8. Hoc, N.Q.; Tinh, B.D.; Hien, N.D. Stress-strain curve of FCC interstitial alloy AuSi under pressure. *Rom. J. Phys.* **2020**, *65*, 608.
9. Hoc, N.Q.; Tinh, B.D.; Coman, G.; Hien, N.D. On the melting of alloys FeX (X = Ni, Ta, Nb, Cr) under pressure up to 5 GPa. *J. Phys. Soc. Jpn.* **2020**, *89*, 114602. [CrossRef]
10. Dung, N.T. Influence of impurity concentration, atomic number, temperature and tempering time on microstructure and phase transformation of Ni1-xFex (x = 0:1, 0.3, 0.5) nanoparticles. *Mod. Phys. Lett. B* **2018**, *32*, 1850204. [CrossRef]
11. Tuan, T.Q.; Dung, N.T. Effect of heating rate, impurity concentration of Cu, atomic number, temperatures, time annealing temperature on the structure, crystallization temperature and crystallization process of Ni1-xCux bulk; x = 0.1, 0.3, 0.5, 0.7. *Int. J. Mod. Phys. B* **2018**, *32*, 1830009. [CrossRef]
12. Nguyen-Trong, D.; Pham-Huu, K.; Nguyen-Tri, P. Simulation on the factors affecting the crystallization process of FeNi alloy by molecular dynamics. *ACS Omega* **2019**, *4*, 14605–14612. [CrossRef] [PubMed]
13. Nguyen-Trong, D.; Nguyen-Chinh, C.; Duong-Quoc, V. Study on the effect of doping on lattice constant and electronic structure of bulk AuCu by the density functional theory. *J. Multiscale Model.* **2020**, *11*, 2030001. [CrossRef]
14. Nguyen-Trong, D.; Nguyen-Tri, P. Factors affecting the structure, phase transition and crystallization process of AlNi nanoparticles. *J. Alloy. Compd.* **2020**, *812*, 152133. [CrossRef]
15. Nguyen-Trong, D.; Nguyen-Tri, P. Molecular dynamic study on factors influencing the structure, phase transition and crystallization process of NiCu6912 nanoparticle. *Mater. Chem. Phys.* **2020**, *250*, 123075. [CrossRef]
16. Long, V.C.; Quoc, V.D.; Trong, D.N. Ab initio calculations on the structural and electronic properties of AgAu alloys. *ACS Omega* **2020**, *5*, 31391–31397. [CrossRef] [PubMed]
17. Trong, D.N.; Long, V.C.; Ţălu, Ş. The structure and crystallizing process of NiAu alloy: A molecular dynamics simulation method. *J. Compos. Sci.* **2021**, *5*, 18. [CrossRef]
18. Nguyen-Trong, D. Z-AXIS deformation method to investigate the influence of system size, structure phase transition on mechanical properties of bulk nickel. *Mater. Chem. Phys.* **2020**, *252*, 123275. [CrossRef]
19. Quoc, T.T.; Trong, D.N.; Ţălu, Ş. Study on the influence of factors on the structure and mechanical properties of amorphous aluminium by molecular dynamics method. *Adv. Mater. Sci. Eng.* **2021**, *5564644*, 1–10. [CrossRef]
20. Kraftmakher, Y. Equilibrium vacancy and thermal property of metals. *Phys. Rep.* **1998**, *299*, 79–198. [CrossRef]
21. Siegel, R.W. Vacancy concentrations in metals. *J. Nucl. Mater.* **1978**, *69–70*, 117–146. [CrossRef]
22. Maier, K.; Peo, M.; Saile, B.; Schaefer, H.E.; Seeger, A. High-temperature positron annihilation and vacancy formation in refractory metals. *Philos. Mag. A* **1979**, *40*, 701. [CrossRef]
23. Pamato, M.G.; Wood, I.G.; Dobson, D.P.; Hunt, S.A.; Vocadlo, L. The thermal expansion of gold: Point defect concentrations and pre-melting I a face-centered cubic metal. *J. Appl. Crystallogr.* **2018**, *51*, 470–480. [CrossRef]
24. Hung, V.V.; Hai, N.T. Investigation of the thermodynamic properties of anharmonic crystals with defects and influence of anharmonicity in EXAFs by the moment method. *Int. Mod. Phys. B* **1998**, *12*, 191. [CrossRef]

25. Vereshchagin, L.F.; Fateeva, N.S. Melting temperatures of refractory metals at high pressures. *High Temp. High Press.* **1977**, *9*, 619–628.
26. Errandonea, D.; Schwager, B.; Ditz, R.; Gessmann, C.; Boehler, R.; Ross, M. Systematics of transition-metal melting. *Phys. Rev. B* **2001**, *63*, 132104. [CrossRef]
27. Saxen, S.K.; Zhang, J. Thermodynamical and pressure-volume-temperature systematics of data on solids, examples: Tungsten and MgO. *Phys. Chem. Miner.* **1990**, *17*, 45–51. [CrossRef]
28. Moriarty, J.A. Ultra-high pressure structural phase transitions in Cr, Mo and W. *Phys. Rev. B* **1992**, *45*, 2004–2014. [CrossRef]
29. Tang, N.; Hung, V.V. Investigation of the thermodynamic properties of anharmonic crystals by the momentum method, (I) General results for FCC crystals. *Phys. Stat. Sol.* **1988**, *149*, 511. [CrossRef]
30. Tang, N.; Hung, V.V. Investigation of the thermodynamic properties of anharmonic crystals by the momentum method, (II) Comparison of calculations with experiments for inert gas crystals. *Phys. Stat. Sol.* **1990**, *161*, 165. [CrossRef]
31. Tang, N.; Hung, V.V. Investigation of the thermodynamic properties of anharmonic crystals by the momentum method, (III) Thermodynamic properties of the crystals at various pressures. *Phys. Stat. Sol.* **1990**, *162*, 371. [CrossRef]
32. Tang, N.; Hung, V.V. Investigation of the thermodynamic properties of anharmonic crystals by the momentum method, (IV) The limiting of absolute stability and the melting temperature of crystals. *Phys. Stat. Sol.* **1990**, *162*, 379. [CrossRef]
33. Hung, V.V. *Statistical Moment Method in Studying Elastic and Thermodynamic Properties of Crystals*; HNUE Publishing House: Hanoi, Vietnam, 2009.
34. Cuong, T.D.; Anh, P.D. Modification of the statistical moment method for the high-pressure melting curve by the inclusion of thermal vacancies. *Vacuum* **2020**, *179*, 109444. [CrossRef]
35. Hung, V.V. Investigation of the change in volume, entropy and specific heat for metals on melting. In Proceedings of the 22nd National Conference of Theoretical Physics, Do Son, Vietnam, 3–5 August 1997; pp. 199–203.
36. Good, R.J.; Hope, C.J. New combining rule for intermolecular distances in intermolecular potential functions. *J. Chem. Phys.* **1970**, *53*, 540–543. [CrossRef]
37. Graf, M.J.; Greeff, C.W.; Boettger, J.C. High-pressure Debye-Waller and Grüneisen parameters of gold and copper. *AIP Conf. Proc.* **2004**, *706*, 65–68.
38. Girifalco, L.A. *Statistical Physics of Materials*; John Wiley & Sons: Hoboken, NJ, USA, 1973.
39. Magomedov, M.N. On calculating the Debye temperature and the Gruneisen parameter. *Z. Fiz. Khimii* **1987**, *61*, 1003–1009. (In Russian)
40. Guo, Z.; Yuan, W.; Sun, Y.; Cai, Z.; Qiao, Z. Thermodynamic assessment of the Si-Ta and Si-W systems. *J. Phase Equilibria Diffus.* **2000**, *30*, 564–570. [CrossRef]